Applied Physics Express

The Japan Society of Applied Physics

Large Interface Spin-Asymmetry and Magnetoresistance in Fully Epitaxial $Co_2MnSi/Ag/Co_2MnSi$ Current-Perpendicular-to-Plane Magnetoresistive Devices

To cite this article: Taku Iwase *et al* 2009 *Appl. Phys. Express* **2** 063003

Applied Physics Express 2 (2009) 063003

Large Interface Spin-Asymmetry and Magnetoresistance in Fully Epitaxial $Co_2MnSi/Ag/Co_2MnSi$ Current-Perpendicular-to-Plane Magnetoresistive Devices

Taku Iwase, Yuya Sakuraba*, Subrojati Bosu, Kesami Saito, Seiji Mitani, and Koki Takanashi

Institute for Materials Research, Tohoku University, Sendai 980-8577, Japan

Received April 3, 2009; accepted May 6, 2009; published online May 29, 2009

Current-perpendicular-to-plane giant magnetoresistance (CPP-GMR) characteristics were investigated in a Co_2MnSi (CMS)/Ag/CMS fully epitaxial device and compared to those in a CMS/Cr/CMS device systematically. Reflection high-energy electron diffraction and transmission electron microscopy images showed the two samples had no remarkable differences and little interdiffusion. The large spin-asymmetry of electron scattering was found at the CMS/Ag inteface compared with that at the CMS/Cr interface. Finally, the largest magneto-resistance (MR) ratio of 28.8% was observed at room temperature in the CMS/Ag/CMS CPP-GMR device.

DOI: 10.1143/APEX.2.063003

Recently, current-perpendicular-to-plane giant magneto-resistance (CPP-GMR) has been extensively studied, because it satisfies an important requirement for next generation magnetic read heads for high-density hard disk drive (HDD) applications, i.e., a small resistance area product (*RA*) suitable for high-speed reading.[1] However, the biggest drawback of CPP-GMR devices is the small magneto-resistance (MR) ratio due to the significant contribution of spin-independent electron scattering to the total resistance in metallic multilayer systems. It is important challenge to improve MR ratio in CPP-GMR devices in order to apply them to a magnetic read head.

Theoretical studies have predicted that some full-Heusler alloys, including Co_2MnSi (CMS) and Co_2MnGe, have 100% spin-polarized conduction electrons (called half-metallicity).[2] Hence, these alloys have attracted much interest in the spintronics field, especially as ferromagnetic electrodes for magnetic tunnel junctions (MTJs) and CPP-GMR devices. Extremely large MR ratios over 100%, which indicate a half-metallic nature, have been already reported in MTJs using Heusler alloy electrodes.[3–6] Moreover, CPP-GMR devices fabricated using half-metallic Heusler alloys have been attempted extensively.[7–11] Saito *et al.* have reported a large MR ratio of 11.5% in dual spin-valve CPP-GMR using Co_2MnGe,[7] and Mizuno *et al.* have demonstrated an MR ratio of 9.0% in a CMS/Cu/CMS single spin-valve structure.[8] In these works, however, an origin for the enhancement of CPP-GMR properties, i.e., large resistivity of Heusler alloy or large spin-asymmetry of electron scattering, has not been clarified. Our recent study on an epitaxially grown (001)-CMS/Cr/CMS CPP-GMR structure has reported an enhanced spin-scattering asymmetry and MR ratio by partially promoting the $L2_1$ chemical ordering in CMS electrodes, suggesting an improved half-metallicity by $L2_1$-ordering.[11] This result implies that a higher $L2_1$ chemical ordering in both the upper and lower CMS electrodes are necessary to improve the spin-asymmetric scattering and obtain a larger MR ratio. Therefore, the interdiffusion between the CMS electrode and a nonmagnetic (NM) interlayer is a critical problem because CMS must be annealed between 700 and 900 K to obtain a high $L2_1$ chemical ordering in general. Ag has potential as the NM layer because it has a small solubility in CMS and good lattice matching with the (001)-plane of CMS (misfit ~2.2%). Herein the structural and CPP-GMR characteristics in a CMS/Ag/CMS fully epitaxial structure are investigated and systematically compared to those in CMS/Cr/CMS structures. The larger ΔRA and MR ratio originate from the large interface spin-asymmetry at CMS/Ag, which is clearly observed in CMS/Ag/CMS structures.

CMS/Ag/CMS and CMS/Cr/CMS fully epitaxial films were prepared by an ultrahigh vacuum (UHV)-compatible magnetron sputtering system ($P_{base} < 1 \times 10^{-7}$ Pa). First, a Cr (20 nm) buffer layer was deposited on a MgO(001) single crystal substrate at room temperature (RT), and subsequently annealed at 973 K to improve the surface flatness. Then a Ag (40 nm)/Cr (10 nm) buffer layer was deposited at RT. The lower CMS layer (8.8 nm) was grown at RT on the Cr/Ag/Cr buffer layer using the $Co_{43.7}Mn_{28.0}Si_{28.4}$ composition alloy target. After deposition, the CMS layer was annealed at 623 K for 10 mins to improve the chemical ordering. Electron probe microanalysis (EPMA) showed a nearly stoichiometric Co–Mn–Si composition in the CMS layer (Co : Mn : Si = 50.4 : 25.0 : 24.6). The Ag (5 nm) or Cr (5 nm) spacer layer and the upper CMS (8.8 nm) layer were deposited after cooling to RT. Then the film was annealed at 623 K, and finally the film was capped by Ag (2 nm)/Au (5 nm) layers. The film was patterned into pillars for CPP-type four-terminal device structures using electron beam lithography and Ar ion milling. The designed size of the pillar changed from 100×200 to $300 \times 600\,nm^2$ on one substrate. The side walls of the pillars were insulated using AlO_x, and Cu/Au was deposited by ion beam sputtering as the upper electrode. The MR characteristics were measured by the DC four-terminal method by applying magnetic field to the easy axis (⟨110⟩ direction) for the CMS layers. In this paper, the samples with Ag spacer and Cr spacer are referred to as "Sample Ag" and "Sample Cr", respectively.

Figure 1 shows reflection high-energy electron diffraction (RHEED) images of the spacer layers, and the lower and upper CMS layers. The images for CMS layers were taken after annealing. Clear streak patterns, representing fully epitaxial growth, were observed in all images. In the RHEED images of Figs. 1(a), 1(b), 1(e), and 1(f), the arrows note streaks associated with $L2_1$-superlattice structure. The superlattice streaks for samples Ag and Cr had

*E-mail address: y.sakuraba@imr.tohoku.ac.jp

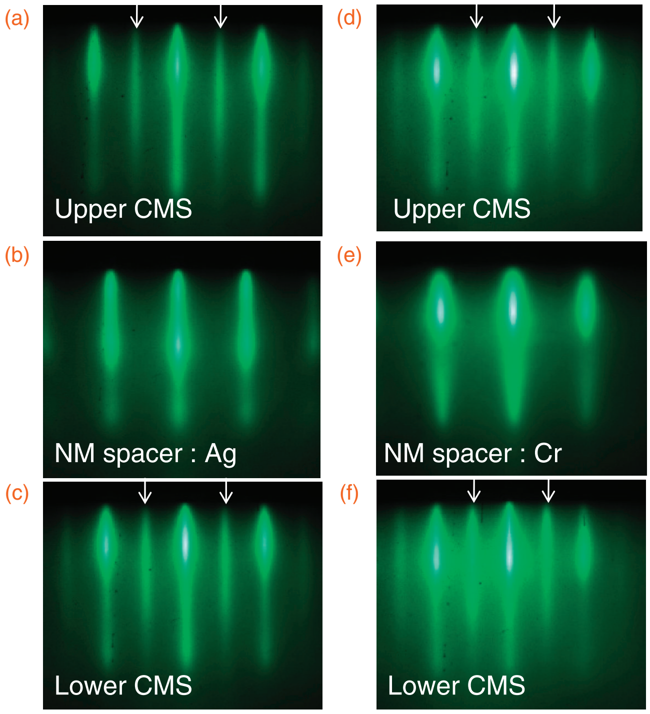

Fig. 1. RHEED images for Samples Ag (a)–(c) and Cr (d)–(g) in the azimuth of the [100] direction for MgO substrates. Images (a), (c) and (d), (g) represent the upper and lower CMS, respectively. Images (b) and (e) are for the Ag and Cr interlayers, respectively. The magnification is not same for each image.

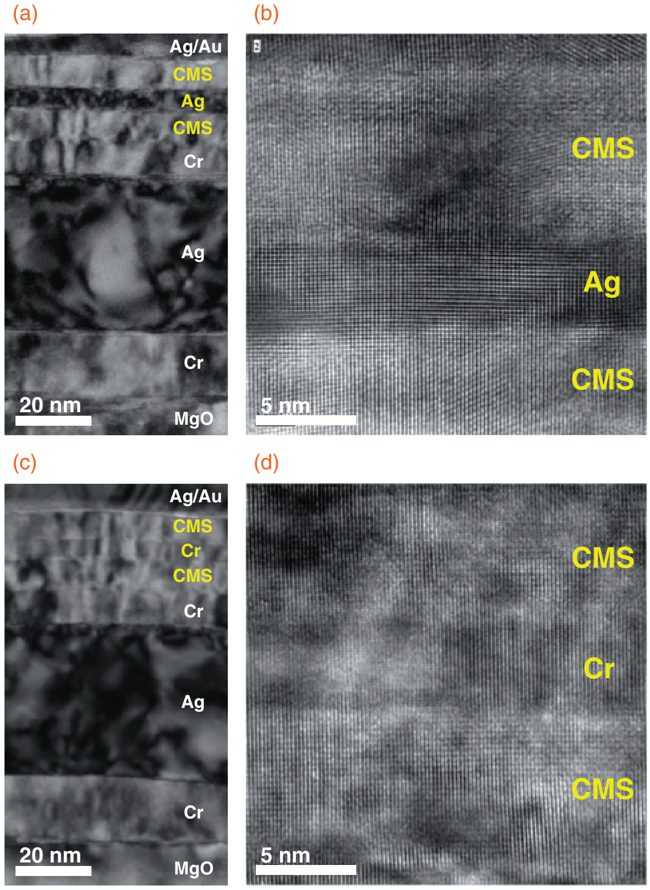

Fig. 2. Cross-sectional TEM images for Samples Ag (a), (b) and Cr (c), (d).

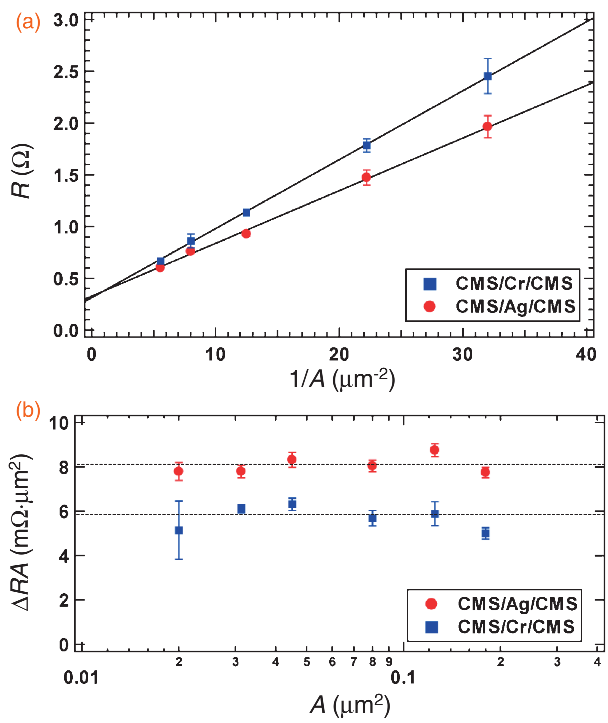

Fig. 3. Pillar size A dependence of RA (a) and ΔRA (b). The broken lines in (b) represent average ΔRA for each sample.

similar sharpness and strengths, suggesting similar degrees of $L2_1$-ordering. Additionally, the RHEED images confirmed samples Ag and Cr do not have remarkable structural differences.

Figure 2 shows bright-field transmission electron microscopy (TEM) images of Samples Ag and Cr. All the layers in both samples had flat interfaces [Figs. 2(a) and 2(c)]. The high-resolution TEM images around CMS/NM/CMS interfaces [Figs. 2(b) and 2(d)] showed excellent epitaxial growth, which agree with RHEED images. It should be noted that in this study both the lower and upper CMS layers were annealed at 623 K, which is a sufficiently low temperature to prevent interdiffusion between the CMS and NM layers. Figures 2(b) and 2(d) confirm the good interface sharpness. The lack of remarkable structural differences between the two samples and the small interdiffusion excluded contributions to the CPP-GMR properties in the following discussion.

Figure 3(a) shows the relationship between pillar size A and resistance R. The $1/A$ dependence of R showed a linear relationship, which implies a micro-fabrication process with a high yield. The average estimated RA values for Samples Ag and Cr were 51.4 and 66.9 $\mathrm{m\Omega \cdot \mu m^2}$, respectively. The nonzero resistance at $1/A = 0$ in Fig. 3 represents the resistance of top and bottom electrodes which does not depend on the pillar size. RA for Sample Ag was smaller than that for Sample Cr by approximately 15.5 $\mathrm{m\Omega \cdot \mu m^2}$. This reduction of RA value is too large to be explained only by the difference in the resistivities of the Ag and Cr interlayer because the resistivity-thickness product for the Cr interlayer ($\rho_{Cr} t_{Cr}$) was less than 3 $\mathrm{m\Omega \cdot \mu m^2}$ even if ρ_{Cr} is five times larger than the bulk resistivity. Hence, the small interface resistance in CMS/Ag ($R_{CMS/Ag}$) compared to that in CMS/Cr ($R_{CMS/Cr}$) contributed to the reduction.

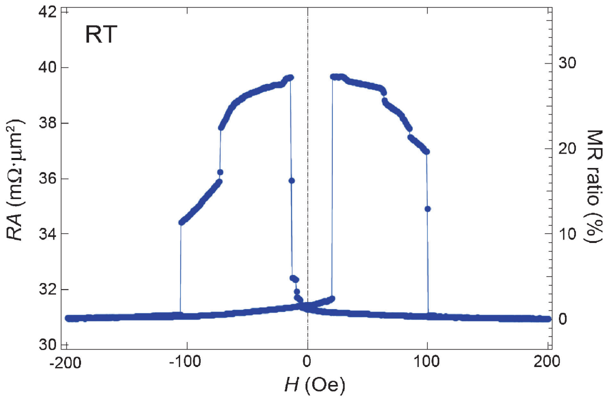

Fig. 4. The MR curve showing maximum MR ratio at RT for a CMS/Ag/CMS CPP-GMR device.

Figure 3(b) shows the pillar size A dependence of the resistance change-area product (ΔRA). The fluctuation of ΔRA was small due to the good micro-fabrication yield ratio. Interestingly, Sample Ag had a larger ΔRA value ($8.76\,\mathrm{m\Omega{\cdot}\mu m^2}$) than Sample Cr ($6.31\,\mathrm{m\Omega{\cdot}\mu m^2}$) in contrast to the smaller RA. The maximum MR ratios of Samples Ag and Cr were 17.2 and 9.7%, respectively.

The origin for the large CPP-GMR for Sample Ag is large spin asymmetry of electron scattering at the CMS/Ag interface as described in the following discussion. In CPP-GMR, ΔRA can be analyzed using Valet and Fert's two-current model.[12] According to their model, spin-dependent electron scatterings in the CMS layers and at the CMS/NM interfaces independently contribute to ΔRA. These bulk and interface effects can be expressed as $\beta\rho_{\mathrm{CMS}}t_{\mathrm{CMS}}/(1-\beta^2)$ and $\gamma AR_{\mathrm{CMS/NM}}/(1-\gamma^2)$, respectively.[13] Here, β and γ are the bulk and interface spin-asymmetry coefficients, respectively; ρ_{CMS} and t_{CMS} are the resistivity and thickness of CMS layer, respectively, and $AR_{\mathrm{CMS/NM}}$ is the resistance-area product at the interface between the CMS and NM layers. It is reasonable to assume that only γ and $AR_{\mathrm{CMS/NM}}$ differ between Samples Ag and Cr due to lack of remarkable differences in structural quality and interdiffusion of these samples. As shown earlier, the RA values for Sample Cr and Ag indicate $AR_{\mathrm{CMS/Cr}} > AR_{\mathrm{CMS/Ag}}$. Hence, γ at the CMS/Ag interface is clearly larger than that at the CMS/Cr interface, which predominantly contributes to the large ΔRA and MR ratio in the CMS/Ag/CMS CPP-GMR device. Since γ is a parameter defined as $(AR_{\mathrm{FM/NM}(m)} - AR_{\mathrm{FM/NM}(M)})/(AR_{\mathrm{FM/NM}(m)} + AR_{\mathrm{FM/NM}(M)})$ (here, m and M denote minority and majority spin, respectively.), a large γ in CMS/NM structures is anticipated owing to large $AR_{\mathrm{FM/NM}(m)}$ caused by the conductance mismatching in minority spin-band at a half-metal/NM interface. A small interface resistance for majority-spin electron at CMS/Ag ($AR_{\mathrm{CMS/Ag}(M)}$) compared to that at CMS/Cr ($AR_{\mathrm{CMS/Cr}(M)}$), which has been also predicted in a recent first principle calculation,[14] is a possible explanation for the enhancement of γ in CMS/Ag/CMS CPP-GMR devices. Note that, a large interface spin-asymmetry is preferable to apply CPP-GMR device to a magnetic read head because there is a limitation of a total device thickness to fit a read gap length of high density HDDs.

Finally, a CMS/Ag/CMS device with higher annealing temperature for CMS electrodes (773 K for a lower CMS, 723 K for an upper CMS) was fabricated for further enhancement of MR ratio. The maximum MR ratio of 28.8% and ΔRA of $8.92\,\mathrm{m\Omega{\cdot}\mu m^2}$ was observed at RT (Fig. 4), which was originated from not only above-mentioned large γ but also large β caused by promoting $L2_1$-ordering. The observed MR ratio of 28.8% at RT is the best value reported for a CPP-GMR device to date. Compared to previous studies on the CPP-GMR with CoFe electrodes,[15,16] the present results exhibited very large ΔRA and MR ratio, which obviously reflects the half-metallic nature of CMS at RT.

In conclusion, CPP-GMR devices with fully epitaxial CMS/Ag/CMS and CMS/Cr/CMS were fabricated, and the structural and MR properties were investigated systematically. The large interface spin-asymmetry of electron scattering was found at the CMS/Ag interfaces compared to that at the CMS/Cr interface. Finally, a maximum MR ratio of 28.8% at RT was achieved in a CMS/Ag/CMS CPP-GMR device.

Acknowledgments Authors thank Y. Miura and M. Shirai for a valuable discussions. This work was supported by the Nano-Materials Functionality Creation Research Project for Young Scientists in IMR, and a Grant-in-Aid for Scientific Research on Priority Area "Creation and control of spin current" (No. 19048004) and a Grant-in-Aid for Young Scientists B (No. 20760005) from the Ministry of Education, Culture, Sports, Science and Technology, Japan.

1) M. Takagishi, K. Koi, M. Yoshikawa, T. Funayama, H. Iwasaki, and M. Sahashi: IEEE Trans. Magn. **38** (2002) 2277.
2) S. Ishida, S. Fujii, S. Kashiwagi, and S. Asano: J. Phys. Soc. Jpn. **64** (1995) 2152.
3) Y. Sakuraba, M. Hattori, M. Oogane, Y. Ando, H. Kato, A. Sakuma, H. Kubota, and T. Miyazak: Appl. Phys. Lett. **88** (2006) 192508.
4) Y. Sakuraba, J. Nakata, M. Oogane, H. Kubota, Y. Ando, A. Sakuma, and T. Miyazaki: Jpn. J. Appl. Phys. **44** (2005) L1100.
5) S. Tsunegi, Y. Sakuraba, M. Oogane, K. Takanashi, and Y. Ando: Appl. Phys. Lett. **93** (2008) 112506.
6) T. Ishikawa, T. Marukame, H. Kijima, K.-I. Matsuda, T. Uemura, M. Arita, and M. Yamamoto: Appl. Phys. Lett. **89** (2006) 192505.
7) M. Saito, N. Hasegawa, Y. Ide, T. Yamashita, Y. Hayakawa, Y. Nishiyama, M. Ishizone, S. Yanagi, K. Nishimura, and A. Takahashi: Dig. Intermag Conf., 2005, Paper No. FB-02.
8) T. Mizuno, Y. Tsuchiya, T. Machita, S. Hara, D. Miyauchi, K. Shimazawa, T. Chou, K. Noguchi, and K. Tagami: IEEE Trans. Magn. **44** (2008) 3584.
9) K. Yakushiji, K. Saito, S. Mitani, K. Takanashi, Y. K. Takahashi, and K. Hono: Appl. Phys. Lett. **88** (2006) 222504.
10) T. Furubayashi, K. Kodama, H. Sukegawa, Y. K. Takahashi, K. Inomata, and K. Hono: Appl. Phys. Lett. **93** (2008) 122507.
11) Y. Sakuraba, T. Iwase, K. Saito, S. Mitani, and K. Takanashi: Appl. Phys. Lett. **94** (2009) 012511.
12) T. Valet and A. Fert: Phys. Rev. B **48** (1993) 7099.
13) J. Bass and W. P. Pratt, Jr.: J. Phys.: Condens. Matter **19** (2007) 183201.
14) Y. Miura, K. Futatsukawa, S. Nakajima, K. Abe, and M. Shirai: in preparation.
15) H. Yuasa, M. Yoshikawa, Y. Kamiguchi, K. Koi, H. Iwasaki, M. Yakagishi, and M. Sahashi: J. Appl. Phys. **92** (2002) 2646.
16) A. Jogo, K. Ngasaka, T. Ibusuki, Y. Shimizu, A. Tanaka, and H. Ohshima: J. Magn. Magn. Mater. **309** (2007) 80.